Identification of palmitoyl protein thioesterase 1 substrates defines roles for synaptic depalmitoylation

Erica L. Gorenberg[1,2], Helen R. Zhao[1], Jason Bishai[3], Vicky Chou[1], Gregory S. Wirak[1], TuKiet T. Lam[4,5], Sreeganga S. Chandra[1,*]

[1] Departments of Neurology; Neuroscience, Yale University, New Haven, CT 06536
[2] Interdepartmental Neuroscience Program, Yale University, New Haven, CT 06510
[3] Department of Microbial Pathogenesis, Yale University, New Haven, CT 06510
[4] Departments of Molecular Biophysics and Biochemistry, Yale University, New Haven, CT 06520
[5] Keck MS & Proteomics Resource, WM Keck Biotechnology Resource Laboratory, New Haven, CT 06510
* To whom correspondence should be addressed to: sreeganga.chandra@yale.edu; 203-785-6172

Author contributions: ELG, HRZ, VC, and GSW conducted experiments. ELG and SSC designed experiments. ELG and JB performed data analysis. TTL conducted mass spectrometry. ELG and SSC wrote paper. All authors read and edited text.

Highlights

- 10% of palmitoylated proteins are palmitoyl protein thioesterase 1 (PPT1) substrates
- Unbiased proteomic approaches identify 9 broad classes of substrates, including synaptic adhesion molecules and endocytic proteins
- PPT1 depalmitoylates several transmembrane proteins in their extracellular domains
- Depalmitoylation allows for disulfide bond formation in some PPT1 substrates
- Protein degradation does not require depalmitoylation by PPT1
- Other palmitoylated Neuronal Ceroid Lipofuscinosis proteins are impacted by deficiency of PPT1, indicating a common disease pathway

Keywords

palmitoylation, synapse, Palmitoyl protein thioesterase 1, neuronal ceroid lipofuscinoisis, neurodegeneration, synaptic adhesion molecules, synaptic vesicle endocytosis, AMPA receptor, synaptic cleft

SUMMARY

We report here the identification of substrates of the depalmitoylating enzyme PPT1 by quantitative mass spectrometry. We first used a stringent Acyl Resin-Assisted Capture (Acyl RAC) screen in which PPT1 knockout (KO) mouse brain proteins showing increased *in vivo* palmitoylation are identified as putative PPT1 substrates. We then validated hits by directly depalmitoylating with PPT1 to confirm *bona fide* substrates. This novel two-step screen identified >100 substrates not previously known to be depalmitoylated by PPT1, including a wide range of channels/transporters, G-proteins, endo/exocytic components, synaptic adhesion molecules, and mitochondrial proteins. Interestingly, many sites of depalmitoylation on transmembrane proteins were located in extracellular domains facing the synaptic cleft. For this group of substrates, depalmitoylation appears to facilitate disulfide bond formation. Collectively, these diverse substrates may explain the many facets of *CLN1* disease caused by the loss of PPT1 function.

BACKGROUND

Palmitoylation is the post-translational addition of a C16:0 fatty acid chain to proteins, typically via thioester bond to cysteine residues. Palmitoylation is unique among lipid post-translational modifications (PTMs) in its reversibility—other lipid PTMs typically last a protein's entire lifespan (Magee et al., 1987). Palmitoylation influences protein stability, function, and membrane trafficking. Addition and removal of the palmitoyl tether allows non-membrane proteins to dynamically associate and dissociate from membranes or change subcellular compartment, as well as direct proteins to localize to specific membrane domains (Greaves and Chamberlain, 2007; Greaves et al., 2009; Hayashi et al., 2005; Lin et al., 2009). Palmitoyl groups are added by a family of 23 palmitoyl acyl transferases (PATs or ZDHHCs); (Lemonidis et al., 2015; Mitchell et al., 2006), and are removed by distinct depalmitoylating enzymes – palmitoyl protein thioesterases (PPTs), acyl protein thioesterases (APTs), and α/β-hydrolase domain-containing proteins (ABHD1-17); (Lin and Conibear, 2015; Vartak et al., 2014; Vesa et al., 1995). The reversible nature of palmitate PTMs suggests that tight regulation of the palmitoylation/depalmitoylation cycle is necessary for proper protein function.

Systematic and unbiased proteomics of the mammalian brain have identified over 600 palmitoylated proteins, a high percentage of which are localized to synapses (Collins et al., 2017; Kang et al., 2008; Segal-Salto et al., 2017). These large-scale screens suggest the importance of palmitoylation for synaptic function and neurotransmission. While recent studies have begun to identify the specific PATs that palmitoylate some synaptic proteins (Fukata et al., 2004; Huang et al., 2004), it is still unclear for most proteins which depalmitoylating enzyme facilitates the removal of palmitate PTMs in the brain and at the synapse.

Considering that loss of PPT1 activity is known to impact presynaptic function and cause aberrant palmitoylation in the neurodegenerative disease Neuronal Ceroid Lipofuscinosis (NCL) type 1 (*CLN1*); (Mitchison et al., 1998; Vesa et al., 1995), we hypothesized that PPT1 plays an integral role in synaptic depalmitoylation and function. However, the

physiological substrates of PPT1 are largely unknown, with the exceptions of CSPα, a presynaptic chaperone, Goα, and the mitochondrial F1 ATP synthase subunit O (Bagh et al., 2017; Duncan and Gilman, 1998; Lyly et al., 2007).

In this study, we undertook a proteomic approach to identify PPT1 substrates with the aim of elucidating how PPT1's depalmitoylating function contributes to normal synaptic function. Palmitoylated proteins from wild type (WT) and PPT1 knockout (KO) mouse brains or synaptosomes were isolated and mass spectrometry (MS) was used to compare palmitoylated protein levels. We identified putative PPT1 substrates as those exhibiting significantly upregulated palmitoylation in PPT1 KO synaptosomes compared to WT synaptosomes. We then performed a secondary unbiased screen to validate the putative PPT1 substrates by directly depalmitoylating synaptic proteins with recombinant mouse PPT1. We found that only ~10% of palmitoylated proteins could be acted upon by PPT1. These proteins fall into 9 classes and include ion channels/transporters, G-proteins, endocytic, synaptic adhesion, and mitochondrial proteins. Among these proteins, we identified those linked to other forms of NCL.

RESULTS

Isolation of the proteome and palmitome from WT and PPT1 KO brain

We hypothesized that neuronal substrates of PPT1 exhibit increased palmitoylation in PPT1 KO mouse brain, but not necessarily changed protein levels. Therefore, we designed an experimental workflow to analyze both the proteome and palmitome from the same WT and PPT1 KO brains by MS (**Figure 1A**). This scheme allowed for comparisons across both genotype (WT vs PPT1 KO) and '-omes' (proteome vs palmitome) and utilizes *in vivo* palmitoylation changes to identify PPT1 substrates. Whole brain homogenates from WT and PPT1 KO mice were processed for Acyl RAC, as previously described (Forrester et al., 2010; Henderson et al., 2016). Briefly, disulfide bonds were reduced with tris(2-carboxyethyl)phosphine (TCEP), and resulting free thiols were blocked with N-ethylmaleimide (NEM; **Figure 1Bi**). Palmitate groups were removed with hydroxylamine (HA; **Figure 1Bii**) and the resulting free thiol was bound to thiopropyl sepharose beads (**Figure 1Biii**) and eluted for Liquid Chromatography (LC) MS/MS (**Figure 1Biv**). Note that only palmitoylated proteins bind thiopropyl sepharose following HA-mediated depalmitoylation (**Figure 1C-D**). Proteome fractions were collected prior to depalmitoylation by HA (**Figure 1A, Bii**), while palmitome fractions were isolated following pulldown (**Figure 1Biv**). Both proteome and palmitome were analyzed by Label-Free Quantification-mass spectrometry (LFQ-MS).

This workflow was conducted on 3 WT and 3 PPT1 KO mouse brains (each in technical triplicate; age = 2 months) in a pair-wise fashion to decrease artifactual changes. We examined proteins common to all 3 experiments, cognizant of the fact that we likely underestimated the number of PPT1 substrates. The resulting MS analysis of the proteome identified 1873 common proteins (**Figure 2A**), and analysis of the palmitome identified 1795 common palmitoylated proteins (**Figure 2C**) in both genotypes. 69.8% of the proteins in the palmitome have been previously validated as palmitoylated or identified

in palmitoylation datasets (SwissPalm); (Blanc et al., 2015). This confirms our ability to successfully identify palmitoylated proteins using Acyl RAC and expands the number of previously known palmitoylated proteins in the brain (Collins et al., 2017; Kang et al., 2008; Segal-Salto et al., 2017).

We first compared across genotypes, evaluating the proteomes (n=1873 proteins) in WT and PPT1 KO brains. Protein expression was highly correlated between WT and PPT1 KO brains (m=0.9802 $\pm$ 0.0023; R^2=0.9916; **Figure S1A**), in line with the lack of overt differences in neurological phenotypes at this age (2 months); (Gupta et al., 2001). Then we analyzed the fold change between genotypes (KO/WT) for the 1873 proteins by volcano plot (**Figure 2B**). We first checked for other known depalmitoylating enzymes – PPT2, APTs, and ABDHs – and found their levels unaltered, suggesting they do not compensate for loss of PPT1 (ABHD12, APT1, APT2; **Figure 2B**, green points). However, there were 5 proteins whose expression levels were significantly increased in PPT1 KO compared to WT (**Figure 2B**). All 5 proteins—ASAH1 (Acid ceramidase), CATD (Cathepsin D), LAMP2 (Lysosomal Associated Membrane Protein 2), SAP (Prosaposin) and TPP1 (Tripeptidyl Peptidase 1)—have been previously shown to be increased in PPT1 KO or *CLN1* models (Chandra et al., 2015; Sleat et al., 2017; Tyynela et al., 1993). Interestingly, TPP1 and CATD mutations cause other forms of NCL, and isoforms of SAP accrue in *CLN1* brains (Tyynela et al., 1993), suggesting a shared disease pathway. Next, we compared the palmitome of WT and PPT1 KO brains and find only 15 proteins that show significantly changed palmitoylation levels (12 increased, 3 decreased; **Figure 2D-E**). As anticipated, we see significantly decreased PPT1 levels in the PPT1 KO – residual levels may be explained by sequence similarity with PPT2. Again, we find increased levels of palmitoylated ASAH1, CATD, SAP and TPP1 in the PPT1 KO reflecting their elevated protein levels. The remaining 8 proteins—SCRB2 (LIMP II), C1QC (Complement C1q subcomponent subunit C), PTTG (Pituitary tumor-transforming gene 1 protein-interacting protein), CATF (Cathepsin F), SRBS1 (Sorbin and SH3 domain-containing protein 1), SRBS2 (Sorbin and SH3 domain-containing protein 2), AP1B1 (AP1 complex Beta-1 subunit), and RTN3 (Reticulon 3)— exhibit only elevated palmitoylation and not expression levels; therefore, they are possible PPT1 substrates.

Most palmitoylated proteins (67.4%) were also identified in the proteome sample (**Figure 2F**), allowing direct comparison of palmitome and total proteome levels. We plotted the ratio of the palmitome to proteome for proteins with significantly increased palmitoylation (**Figure 2G**) in PPT1 KO after normalization to WT, and found that the ratios for the lysosomal proteins ASAH1, CATD, SAP, SCRB2, and TPP1 were unchanged, while those for AP1B1, SRBS1, SRBS2, and RTN3 show elevated palmitoylation relative to protein expression in PPT1 KO brains, indicating the latter proteins were indeed putative substrates (**Figure 2G**). In further support of this conclusion, all but SRBS2 have been previously shown to be palmitoylated (SwissPalm); (Blanc et al., 2015).

Putative Synaptic Substrates of PPT1

Immunocytochemistry of neurons and cell lines shows that PPT1 is enriched at synapses in neurons, while it is largely lysosomal in non-neuronal cell types (Ahtiainen et al., 2002;

Kim et al., 2008; Lehtovirta et al., 2001); (**Figure S2**). As we identified very few palmitoylation changes between WT and PPT1 KO from the whole brain analyses, including PPT1's known substrates CSPα, Goα, and F1 ATPase O subunit (Bagh et al., 2017; Duncan and Gilman, 1998; Lyly et al., 2007), we reasoned that sub-compartmentalization of PPT1 may dilute the LFQ signal. Therefore, we proceeded to isolate synaptosomes (a biochemical synaptic preparation) from WT and PPT1 KO brains to enrich for PPT1 and its potential substrates. We then subjected synaptosomes to the same workflow described for whole brain (**Figure 1B; Figure S3A**). We identified a high degree of overlap between the 3 synaptosomal preparations for the proteome, indicating excellent reproducibility, with 1817 common proteins between all 3 biological replicates (**Figure 3A**). Consistent with a synaptic localization and previous literature, we identified PPT1 in the synaptosomal proteome (**Table S1)**; (Ahtiainen et al., 2002; Kim et al., 2008; Lehtovirta et al., 2001). As with the whole brain, we checked for other depalmitoylating enzymes at the synapse and found their levels unchanged (ABHD12, ABHDA, ABHGA, APT2; **Figure 3B**, green points).

When we compared synaptic proteomes across genotypes, we again found that protein expression between WT and PPT1 KO was highly correlated ($m= 0.969 \pm 0.0016$; $R^2 = 0.9666$; **Figure S3B**). Notably, PPT1 is the only protein with significantly decreased expression in KO synaptosomes (**Figure 3B**). Ten proteins exhibited increased expression in PPT1 KO samples, most of which were also seen in the whole brain analysis (**Figure 2**). The only exceptions were the mitochondrial proteins TOM7, CX7A2, and NDUF4.

In the palmitome, we identified 1378 common proteins (**Figure 3C**). Notably, there was much lower correlation between WT and PPT1 KO palmitomes ($m= 1.134 \pm 0.0197$; $R^2 = 0.8986$; **Figure S3C**), with many (610; 44.3%) points above the y=x unity line indicating elevated palmitoylation in PPT1 KO synaptosomes. This striking increase in palmitoylation in PPT1 KO synaptosomes (**Figure 3**) compared to whole brain (**Figure 2**), strongly indicates that PPT1 is active at synapses.

The proteins of greatest interest as potential PPT1 substrates were those with significantly increased palmitoylation in PPT1 KO compared to WT ($p<0.05$, 1.5-fold change cut-off). We identified 238 such proteins (**Figure 3D-E**; **Table S2**). We filtered these data through the CRAPome, a consolidated database of non-specific protein interactors routinely found in pull-down experiments (Mellacheruvu et al., 2013); (n=9 proteins; **Table S3**). We further narrowed the list of substrates by removing those without a cysteine residue to be palmitoylated (n=2 proteins; **Table S3**). The resulting 227 proteins were considered putative PPT1 substrates and include the previously known substrates, CSPα, F1 ATP synthase subunit O, and Goα (Bagh et al., 2017; Duncan and Gilman, 1998; Lyly et al., 2007). Most of the putative substrates were also identified in the whole brain proteome (77.1%), and palmitome (72.0%; **Figure S1C-D**), but their palmitoylation levels were not significant, likely because of PPT1's synaptic compartmentalization. However, SCRB2 and SRBS2, which were identified as putative PPT1 substrates in the whole brain analysis (**Figure 2D**), were also identified here. These data strongly suggest that PPT1 and its substrates are enriched at the synapse.

To confirm that the putative PPT1 substrates show increased palmitoylation independent of protein expression levels, we first compared by volcano plot. Only 10 proteins, showed significantly increased expression (proteome KO/WT ratio >1.5, P<0.05) in PPT1 KO synaptosomes (**Figure 3B**). Only 4 of these (ASAH1, CATD, TPP1, and SCRB2) also show elevated palmitoylation (**Figure 3D**). The remaining putative substrates (n=223) showed elevated palmitoylation without a commensurate increase in protein levels, indicating they are not being depalmitoylated in PPT1 KO synapses to the same extent they are in WT synapses. Significantly, we also identified dynamin-1, which showed increased Acyl RAC pulldown in the PPT1 KO synaptosomes by Western blotting (**Figure 1C-D**) but not SNAP-25, congruent with these results.

Approximately 66% of proteins present in the synaptic palmitome were also identified in the synaptic proteome (n=1209; **Figure 3F**). We examined the putative substrates by plotting the KO/WT ratio to get a clearer picture of the relationship between palmitoylation and protein levels (**Figure 3F**). In line with our initial analysis (**Figure 3B** and **D**), we found only 5 proteins with increased expression as well as palmitoylation in PPT1 KO synaptosomes: ASAH1, CATD, NNTM, SCRB2, and TPP1 (**Figure 3G,** orange region). For these proteins, the observed increase in palmitoylation reflects protein expression and thus they may not be substrates or may be substrates that exhibit depalmitoylation-dependent degradation. Therefore, they were removed from further consideration (**Table S3**). However, the remaining putative PPT1 substrates identified in both proteome and palmitome show elevated palmitoylation independent of any significant protein expression increase (n=210; blue/white region). The relative increase in palmitoylation in PPT1 KO ranged from 1.5- fold at the lower limit to 2400-fold (Ephrin A4; EphA4) at the upper limit, with known PPT1 substrates CSPα (DNJC5; 5.12-fold), F1ATPase O subunit (ATPO; 3.39-fold) and the Goα subunit (GNAO; 4.81-fold) at 3-5-fold (**Figure 3G**).

Next, we examined the putative PPT1 substrates biochemically for evidence of palmitoylation. By analyzing individual peptides identified in the LFQ-MS for each protein, we inferred cysteine-containing peptides modified with a palmitoyl group. Palmitoylated peptides are identified by their now-derivatized carbamidomethyl moiety where formerly there was a palmitoyl group. Out of 227 putative substrates, we detected 103 proteins (45.4%; **Table S4**) with cysteine peptides modified by a carbamidomethyl group.

We also checked our presumed substrates for prior evidence of palmitoylation. We cross-referenced the 227 putative substrates to 2 databases, one that predicts palmitoylation sites (CSS Palm); (Ren et al., 2008) and one that screens literature for identified and validated palmitoylated proteins (Swiss Palm); (Blanc et al., 2015). In addition, we checked a published analysis of the synaptic palmitome (Kang et al., 2008). By comparing to these datasets, we confirmed that 150 of the 227 proteins are indeed palmitoylated proteins (66.1%; **Table S5**). We also checked if these proteins had been identified in PPT1 interactome datasets (Sapir et al., 2019) and found only 13 of these present (DYL2, DYN1, GABR2, GBB2, KIF5C, LDHB, SSDH, STXB1, SYT2, TERA, THY1, UBA1, and VA0D1). Together, these data comprehensively substantiate that PPT1 substrates are localized to the synapse and can be identified by unbiased comparative approaches.

Secondary validation screen for PPT1 substrates

To validate the putative hits identified in our initial Acyl RAC screen, we developed a modified Acyl RAC protocol using recombinant mouse PPT1 expressed in HEK 293T cells as the depalmitoylating reagent, rather than hydroxylamine. We have previously established that recombinant PPT1 can depalmitoylate its substrate CSPα *in vitro* (Henderson et al., 2016). Concentrated mouse PPT1 was incubated with WT synaptosomes at Step ii of the Acyl RAC protocol (**Figure 1Bii, Figure 4Ai**).

MS analysis of PPT1-depalmitoylated samples identified 975 common proteins over 3 biological replicates (**Figure 4Aii)**, underscoring that PPT1 is moderately specific even *in vitro* and does not depalmitoylate all palmitoylated proteins. 142 of the 227 putative substrates identified in the primary screen were validated (**Figure 4Aiii**). Significantly, investigation of the peptide data showed that we could identify the carbamidomethyl-modified peptide for some of these proteins. Using this information, we categorized the protein hits from the validation screen based on degree of stringency. 1) High confidence PPT1 substrates are those for which matching carbamidomethyl peptides were identified in both the initial Acyl RAC WT/PPT1 KO screen and the PPT1-mediated depalmitoylation validation (n=27; **Table 1**). 2) Medium confidence substrates are those identified in both the primary and validation screen with ≥2 unique peptides and a confidence score >100 (n=115; **Table 2**). 3) Low confidence substrates were those not identified in the validation screen (n=85; **Table S6**). 4) Residuals were proteins identified as potential substrates that were identified only in the second screen and not in the primary screen (n=613; **Table S7**). Notably, most of the high- and medium-confidence PPT1 substrates have been identified in Swiss Palm and/or CSS Palm as palmitoylated by other groups. (**Tables 1, 2, S5**). This list includes all known PPT1 substrates – CSPα, Goα, and F1 subunit O of mitochondrial ATP synthase. It also excludes proteins that have been identified as substrates of other depalmitoylating enzymes; for example, PSD-95, an abundant synaptic protein that is exclusively depalmitoylated by ABHD17 (Yokoi et al., 2016). Putative APT1 substrates such as RAB9A, RAB6A, N-RAS, R-RAS, GAP-43, and SNAP-23 are also excluded (Duncan and Gilman, 1998; Kong et al., 2013; Liu et al., 2019).

Classification of synaptic substrates and functions

To gain insight into the role PPT1 depalmitoylation may play at the synapse, we examined the sub-synaptic location of the high-confidence substrates. We find that most proteins are localized to the synaptic plasma membrane (15/27) with the remaining in the synaptic cytosol (6/27) or at organelles such as mitochondria and lysosomes (6/27; **Table S8**). None of these proteins are localized solely to the post-synaptic cytosol. Furthermore, we looked for the carbamidomethyl-modified cysteine identified for high-confidence PPT1 substrates to identify common features. To our surprise, we find that the carbamidomethyl peptides for most membrane-associated substrates are extracellular, facing the synaptic cleft (**Table S8**). There is strong prior evidence for extracellular palmitoylation (Janda and Garcia, 2015; Kim et al., 2018; Miura and Treisman, 2006; Naschberger et al., 2017; Romancino et al., 2018; Yu et al., 2017) consistent with palmitoylation occurring in the

lumen of the ER or Golgi by the DHHCs resident there (ER PATs: DHHC4, DHHC6, DHHC9, DHHC16; potential Golgi PATs: DHHC3, DHHC21). The identification of GPI-anchored substrates (THY1 and NTRI) further supports the premise that PPT1 depalmitoylation occurs in the synaptic cleft (**Figure 5A**). We additionally find AT1B1 and AT1B2, proteins expressed on astrocytic membranes juxtaposed to the synapse. Strikingly, we find that for all 12 peptides identified as extracellular and carbamidomethyl-modified, the modified cysteines form disulfide bonds in the mature protein (**Table S8**). This suggests that cysteines could be shared for palmitoylation and disulfide bond formation, and that intracellular palmitoylation precedes disulfide bond formation as proposed previously (Bechtel et al., 2020; Itoh et al., 2018; Yu et al., 2017). Many of the proteins containing these extracellular peptides fall into the broad classes of adhesion molecules (NFASC, NRCAM, CADM2, NTRI, THY1, BASI), and channels/transporters (GRIA1, AT1B1, AT1B2; **Figure 4B**). Overall, PPT1 depalmitoylates both intracellular and extracellular substrates.

To obtain a better understanding of the role of PPT1-dependent depalmitoylation, we grouped the high- and medium-confidence PPT1 substrates into 9 distinct functional classes using UniProt Gene Ontology: 1) Cytoskeletal proteins (n=13) 2) Lysosomal proteins (n=2); 3) Mitochondrial proteins (n=23); 4) Synaptic adhesion molecules (n=10); 5) Channels and transporters (n=18); 6) Kinases and phosphatases (n=6); 7) Exo- and endocytic proteins (n=15); 8) Membrane proteins (n=7); 9) G-proteins (n=11); and 10) Other proteins (n=35; **Figure 4B**). Notably, most high- and medium-confidence validated proteins (75%) fall nicely into defined functional classes, indicating that PPT1 primarily influences related functions at the synapse. Literature suggests that palmitoylation regulates function of several of these protein classes, including ion channels and transporters, G-proteins, and mitochondrial proteins (Goddard and Watts, 2012; Montersino and Thomas, 2015; Shipston, 2011). Our findings that synaptic adhesion molecules, endocytic proteins and other lysosomal storage disease-linked proteins are regulated by depalmitoylation are novel. Strikingly, the PPT1 substrate classes reflect the phenotypes observed in PPT1 KO mice and *CLN1* patients, including seizures, decreased synapse density, mitochondrial dysfunction, and synaptic vesicle endocytic deficits (Gupta et al., 2001; Kim et al., 2008; Sapir et al., 2019; Virmani et al., 2005; Wei et al., 2011). Several substrates such as NRCAM2 were also identified in a genetic modifier screen of *Drosophila* PPT1 KO-induced degeneration (Buff et al., 2007).

We used Ingenuity Pathway Analysis (IPA) to determine the functional pathways of the high- and medium-confidence PPT1 substrates in an unbiased manner. The top pathways identified were (1) GABA receptor signaling, (2) CREB signaling in neurons, (3) Synaptic long-term depression, (4) Endocannabinoid neuronal synapse pathway, and (5) Synaptogenesis signaling pathway (**Figure 4C**). These functional pathways are consistent with the 9 functional classes we defined. Notably, pathway analysis of the entire synaptic proteome included only synaptogenesis signaling pathway in its top 5 affected pathways, demonstrating that enrichment for synaptic proteins alone does not lead to the changes exhibited in the palmitome.

Search for Structural Motifs

Since we find that PPT1 is moderately specific and confirmed that it can depalmitoylate 142 proteins *in vivo* (~10% of the WT synaptic palmitome), we wanted to investigate possible determinants of its specificity. Therefore, we carried out three sets of independent analyses. First, we compared the primary sequences of the 31 high-confidence substrates and drew Logo plots. However, we did not observe any striking motifs besides the conserved cysteine (**Figure S4**), suggesting that various classes of PPT1 substrates may have different recognition sites. We next aligned the sequences flanking the carbamidomethyl peptide in cell adhesion and ion transporter classes of proteins, since these classes have several high-confidence substrates. We discovered that the synaptic adhesion PPT1 substrates are conserved and belong to the Immunoglobulin (Ig) domain containing class of homotypic adhesion molecules (**Figure 5A**). The best characterized of these are CADM2 (SynCAM) and NRCAM. Based on their structures, we identified that the carbamidomethyl peptides in most proteins map to one of two crucial cysteines in extracellular IgG domains (**Figure 5B-C**); (Fogel et al., 2010). The palmitoylated cysteines are on exposed and accessible beta-strands and normally form intra-domain disulfide bonds to maintain the typical IgG domain fold (**Figure 5C**). The palmitoylated cysteines identified in the other synaptic adhesion molecules are known to mediate intra or intermolecular interactions via disulfide bonds (Fogel et al., 2011). Overall, our data suggest that PPT1 can recognize the IgG fold.

We have identified that the PPT1 depalmitoylation site for the GluA1 AMPA receptor subunit (GRIA1) is also on the extracellular domain. This extracellular site has not been previously identified, though other palmitoylation sites have been previously identified (Herguedas et al., 2019). The site we identified, (C323) typically forms a disulfide bond (to C75). AMPA receptor subunit palmitoylation is known to regulate sensitization as well as localization (Hayashi et al., 2005; Itoh et al., 2018). From the recent crystal structure (Herguedas et al., 2019), the PPT1-depalmitoylated cysteine is an exposed loop, so accessibility of the cysteine appears to be a key feature.

Next, we tested whether partner palmitoylating enzymes are the primary determinant for PPT1 substrate recognition. Two DHHC/PATs, DHHC5 and DHHC17, localize to synapses (Li et al., 2010; Pandya et al., 2017). DHHC17 and its fly homolog, HIP-14, are known to traffic many synaptic proteins in a palmitoylation dependent manner, including CSPα (Greaves et al., 2008). DHHC17 is the only PAT with a known substrate-recognition motif (Lemonidis et al., 2015). Its recognition sequence is ([VIAP][VIT]xxQP) is usually adjacent to the cysteine that is palmitoylated. We screened the 142 validated PPT1 substrates for the DHHC17 recognition motif and identified 9 cytosolic proteins with this motif, including CLH1 (Clathrin heavy chain), DYN1 (Dynamin 1), SYNJ1 (Synaptojanin 1), and DNJC5 (CSPα) (**Tables 1-2**; **Figure S4**). This subset of PPT1 substrates identified "Clathrin-mediated endocytosis signaling" as the top pathway by IPA (**Figure 5D**), consistent with the known function these proteins play in synaptic vesicle endocytosis (Saheki and De Camilli, 2012). This suggests for the endocytic class of PPT1 substrates, that DHHC17 recognition site is the determinant of substrate specificity.

DISCUSSION

We have systematically and quantitatively characterized palmitoylation in WT and PPT1 KO mice to identify PPT1 substrates. The broad and quantitative nature of our approach has not only identified PPT1 substrates but also illuminated the functions of depalmitoylation at the synapse. Here, we highlight the most salient insights revealed by our analysis to encourage others to use this resource in their own investigations.

Brain and Synaptic Palmitomes

In this study, we present a comprehensive data-set on the brain (n=1795) and synaptic palmitomes (n=1378). This is the largest mouse brain palmitome to date and is a valuable resource to the community (PRIDE accession PXD017270).

PPT1 substrates

As the end result of our two-step screen, we identified 142 high- to medium-confidence PPT1 substrates. We are confident these are *bona fide* substrates because of the stringent nature of our selection process: 1) Inclusion of only proteins that were independently identified in 3 biological samples with robust identification measures (>2 unique peptides); 2) Utilization of *in vivo* differences (KO/WT >1.5; $p<0.05$) as the initial criteria for selection (**Figure 2, Figure 3**); 3) Independent validation by direct PPT1 enzymatic depalmitoylation (**Figure 4**); 4) Previously published PPT1 substrates were validated; 5) Palmitoylated proteins that are known to be exclusively depalmitoylated by AHBD-17 or APT1 were not identified, indicating specificity; 6) The PPT1 substrates cluster into known functional groups (**Figure 4**); 7) Synaptic adhesion molecules and endocytic PPT1 substrates have common structural motifs that explain substrate specificity (**Figure 5**).

As with any proteome-wide screen, a fraction of substrates was likely not identified, such as low confidence and residual hits (**Table S5-S6**) and should be re-examined in a case-by-case manner. This is particularly true for the few proteins (n=4; ASAH1, CATD, TPP1, and SCRB2; **Table S3**) whose expression and palmitoylation both increased significantly and could not be defined as PPT1 substrates. It is possible that these proteins exhibit palmitoylation-dependent degradation, as has been previously suggested to explain lipidated protein accumulation in *CLN1* disease (Hofmann et al., 1997). Alternatively, their increased expression may highlight a common mechanism in lysosomal storage disorders.

Our data indicate that PPT1 is a moderately selective enzyme that depalmitoylates ~10% of the synaptic palmitome, while other depalmitoylating enzymes (APTs, ABHDs) depalmitoylate the remaining substrates. PPT1 and other depalmitoylating enzymes may have overlapping substrates, however, our results suggest this is uncommon, as APTs and ABHDs do not compensate for loss of PPT1 (**Figure 2B, 3B**). The severity and early onset of *CLN1* disease also points to specificity of PPT1 for its substrates.

Functions of synaptic depalmitoylation

Analysis of PPT1 substrates across the 9 functional groups suggests a shared role for depalmitoylation in synaptic protein trafficking. Previous literature has established that palmitoylation of synaptic proteins is essential for their trafficking from the soma to the nerve terminal (i.e. Fukata and Fukata, 2010; Kanaani et al., 2004). The palmitoylation of synaptic proteins destined for the secretory pathway is accomplished by resident PATs in the lumen of the ER or Golgi (Bechtel et al., 2020), while for other proteins, palmitoylation occurs on the cytosolic surface of these organelles. Though the precise PATs serving these distinct roles are not known, palmitoylation facilitates sorting (secretory) and hitching (cytosolic) of synaptic proteins to the synaptic vesicle precursor membrane (Greaves and Chamberlain, 2007; Hayashi et al., 2005). We speculate that besides keeping synaptically targeted proteins tethered to vesicles, palmitoylation is important for keeping synaptic proteins inert during axonal trafficking, i.e. preventing formation of disulfide bonds, and hence, ectopic adhesion interactions or enzymatic activity. Once at the synapse, cytosolic proteins (such as G-proteins, endocytic proteins, kinases, and phosphatases) need to be released from the synaptic vesicle precursor, while membrane proteins (synaptic adhesion molecules) need to be inserted into the synaptic membrane and interact in both *cis* and *trans*. Our results suggest that local synaptic depalmitoylation by PPT1 serves these functions. In the case of membrane proteins with extracellular depalmitoylation, it is likely that the depalmitoylated cysteines spontaneously form disulfide bonds in the oxidative extracellular environment, leading to functional maturation (Bechtel et al., 2020; Cijsouw et al., 2018). In PPT1 KO neurons, palmitoylated synaptic proteins traffic correctly (as PATs are normal, hence the very few changes in the synaptic proteome; **Figure 3B**), however they function poorly at the synapse due to absent or compromised depalmitoylation (**Figure 3D**).

Our findings on PPT1-mediated depalmitoylation of IgG domains in cell adhesion molecules also suggest an important role for PPT1 in regulating synaptogenesis (**Figure 5A-C**). This finding correlates with the “Synaptogenesis signaling pathway” identified by IPA as impacted by palmitoylation in PPT1 KO (**Figure 4C**), as well as previous findings on the importance of NrCAM palmitoylation for neuronal morphogenesis (Ponimaskin et al., 2008). The aberrant palmitoylation of IgG-class adhesion molecule substrates may explain previously-described post-synaptic deficits, including immature dendritic spine morphology of cultured neurons (Koster and Yoshii, 2019; Sapir et al., 2019). Additional research on adhesion molecule depalmitoylation in development may elucidate whether these changes are due to failed cis/trans assembly.

Our results highlight the importance of investigating PPT1 trafficking in neurons in order to further elucidate how PPT1 regulates its substrates. Based on the substrates we have identified, it appears that PPT1 is secreted, endocytosed and then retrogradely trafficked to endosomes/lysosomes as previously described in non-neuronal cells (Hellsten et al., 1996). PPT1 is known to be trafficked along axons to synapses, possibly in synaptic vesicles (**Figure S2; Figure 6**); (Ahtiainen et al., 2002; Lehtovirta et al., 2001) and we suggest it is likely released into the synaptic cleft. This provides a mechanism for how PPT1 can regulate both pre- and post-synaptic ion channels, transporters, and synaptic adhesion molecules (**Figure 6**). This makes PPT1 an important synaptic cleft enzyme.

Once endocytosed into the presynaptic terminal, a fraction of PPT1 appears to escape and access cytosolic substrates – how this is achieved is an exciting question in protein trafficking. One unexplored possibility is that a palmitoyl tether on PPT1 allows for flip-flop across the membrane. Alternatively, there may be two pools of PPT1- one that is exocytosed and another that is not trafficked through the secretory pathway and remains in the presynaptic cytosol. Overall, identification of PPT1 substrates has opened stimulating new avenues for further research to investigate how this PTM regulates synaptic function.

Palmitoylation-depalmitoylation cycles at the synapse

The PATs DHHC5 and DHHC17 have been described to function locally and continuously to palmitoylate synaptic substrates (Fukata et al., 2004; Sialana et al., 2016). We documented a likely DHHC17-PPT1 partnership for palmitoylation-depalmitoylation cycles at the synapse (**Figure 5D-E**) by identifying 9 proteins containing the DHHC17 recognition motif ([VIAP][VIT]xxQP); (Lemonidis et al., 2015). These include CLH1, DYN1, and SYNJ1, and DNJC5 (**Table S2**), which have known functions in synaptic vesicle recycling (**Figure 5D**); (Ferguson et al., 2007; Hinshaw, 2000; Newton et al., 2006; Royle and Lagnado, 2010; Umbach et al., 1994; Verstreken et al., 2003; Zhang et al., 2012; Zinsmaier et al., 1994). Strikingly, previous studies have identified synaptic vesicle endocytosis deficits in PPT1 KO neurons (Virmani et al., 2005), including reduced pre-synaptic vesicle pool size, deficits in evoked pre-synaptic vesicle release (Kim et al., 2008; Virmani et al., 2005), and the persistence of VAMP2 and SNAP25 on the presynaptic membrane (Kim et al., 2008). We hypothesize that palmitoylation-depalmitoylation dynamics regulated respectively by DHHC17 and PPT1, allow for efficient membrane association and dissociation of endocytic proteins during synaptic vesicle endocytosis. However, the exact timing of palmitoylation and depalmitoylation and the triggers for this cycle remain to be clarified. Identification of motifs recognized by DHHC5 may provide additional insights into local regulation of other PPT1 substrates. Overall, it appears that cycles of palmitoylation and depalmitoylation occur locally at the synapse.

Elucidating the relationship between PPT1 protein depalmitoylation and protein degradation.

Due to its link to NCL and lysosomal storage diseases more broadly, PPT1 depalmitoylation activity has long been considered necessary for protein degradation (Koster and Yoshii, 2019; Lu et al., 1996). The original description of cellular phenotypes of *CLN1* included the accumulation of lipid modified cysteine-containing peptides/proteins in patient-derived lymphocytes and skin fibroblasts (Hofmann et al., 1997; Lu et al., 1996). The cysteine-containing proteins modified by palmitoyl thioesters were not identified, although their importance in understanding disease pathogenesis was recognized. Having successfully identified substrates of PPT1, we now re-examine the question of how palmitoylation is related to protein levels by looking only at the 142 validated PPT1 substrates. Counterintuitively, we find that in PPT1 KO, most palmitoylated proteins show significantly increased palmitoylation in PPT1 KO independent of increased protein levels

and exhibit either unchanged or decreased protein expression at the synapse (**Figure 3F**). This analysis suggests that, for most proteins, either the palmitate group does not need to be removed for proteasomal degradation or another depalmitoylating enzyme is responsible for depalmitoylation prior to protein degradation. The group of proteins with increased expression and palmitoylation (**Table S3**) may have increased expression levels or show depalmitoylation-dependent degradation and this remains to be clarified (Qiao et al., 2007). These 4 proteins—ASAH1, TPP1, SAP, CATD—may be the originally described lipidated peptides seen in lipofuscin and needs to be investigated in human tissue.

Role of depalmitoylation in NCLs

We previously showed that patient brains with DNJC5 mutations (*CLN4*) have elevated PPT1 protein levels (Benitez and Sands, 2017; Henderson et al., 2016) but low specific activity, leading to global changes in palmitoylation (Henderson et al., 2016). We have now identified 4 of the proteins exhibiting altered palmitoylation in *CLN4* brains as PPT1 substrates (DYN1, NSF, SYNPR, STXB1, **Table 1-2**), reiterating that *CLN1* and *CLN4* are closely related diseases. Unfortunately, the difficulty in obtaining *CLN1* brains and the devasted state of end-stage brains preclude confirming our results in human samples.

Aberrant palmitoylation has also been identified in other neurodegenerative disorders, such as Huntington's disease. The PAT Huntingtin interacting protein 14 (Hip14), is known to palmitoylate CSPα (Ohyama et al., 2007) and interacts with synaptotagmin VII and GPM6A (Butland et al., 2014; Huang et al., 2004). Interestingly, all three proteins have now emerged as substrates of PPT1 (**Table 1**), suggesting a potential role of depalmitoylation in Huntington's disease as well.

CONCLUSIONS

The identification of the synaptic PPT1 substrates provides a rational basis for investigating fundamental mechanisms that regulate synaptic function. It also establishes a new reference frame for how perturbations of depalmitoylation may contribute to NCL and other neurodegenerative diseases.

Acknowledgments:
This work was supported by NIH (R01 NS064963, R01 NS110354, R01 NS083846, R21 NS094971), and DOD (W81XWH-17-1-0564). The proteomic experiments were supported by the Yale/NIDA Neuroproteomic Center (NIH DA018343). We would like to thank Weiwei Wang and Jean Kanyo for mass spectrometry samples preparation and data collection; and John. E. Lee, Angus Nairn, and Arthur Horwich for editing the manuscript. The Q-Exactive Plus mass spectrometer was funded in part by NIH SIG from the Office of The Director, NIH under award number (S10OD018034).

References:

Ahtiainen, L., Van Diggelen, O.P., Jalanko, A., and Kopra, O. (2002). Palmitoyl protein thioesterase 1 is targeted to the axons in neurons. J Comp Neurol *455*, 368-377.

Bagh, M.B., Peng, S., Chandra, G., Zhang, Z., Singh, S.P., Pattabiraman, N., Liu, A., and Mukherjee, A.B. (2017). Misrouting of v-ATPase subunit V0a1 dysregulates lysosomal acidification in a neurodegenerative lysosomal storage disease model. Nat Commun *8*, 14612.

Bechtel, T.J., Li, C., Kisty, E.A., Maurais, A.J., and Weerapana, E. (2020). Profiling Cysteine Reactivity and Oxidation in the Endoplasmic Reticulum. ACS Chem Biol.

Benitez, B.A., and Sands, M.S. (2017). Primary fibroblasts from CSPα mutation carriers recapitulate hallmarks of the adult onset neuronal ceroid lipofuscinosis. Scientific Reports *7*, 1-15.

Blanc, M., David, F., Abrami, L., Migliozzi, D., Armand, F., Burgi, J., and van der Goot, F.G. (2015). SwissPalm: Protein Palmitoylation database. F1000Res *4*, 261.

Buff, H., Smith, A.C., and Korey, C.A. (2007). Genetic Modifiers of Drosophila Palmitoyl–Protein Thioesterase 1-Induced Degeneration. In Genetics, pp. 209-220.

Butland, S.L., Sanders, S.S., Schmidt, M.E., Riechers, S.P., Lin, D.T., Martin, D.D., Vaid, K., Graham, R.K., Singaraja, R.R., Wanker, E.E.*, et al.* (2014). The palmitoyl acyltransferase HIP14 shares a high proportion of interactors with huntingtin: implications for a role in the pathogenesis of Huntington's disease. Hum Mol Genet *23*, 4142-4160.

Chandra, G., Bagh, M.B., Peng, S., Saha, A., Sarkar, C., Moralle, M., Zhang, Z., and Mukherjee, A.B. (2015). Cln1 gene disruption in mice reveals a common pathogenic link between two of the most lethal childhood neurodegenerative lysosomal storage disorders. Hum Mol Genet *24*, 5416-5432.

Cijsouw, T., Ramsey, A.M., Lam, T.T., Carbone, B.E., Blanpied, T.A., and Biederer, T. (2018). Mapping the Proteome of the Synaptic Cleft through Proximity Labeling Reveals New Cleft Proteins. Proteomes *6*.

Collins, M.O., Woodley, K.T., and Choudhary, J.S. (2017). Global, site-specific analysis of neuronal protein S-acylation. Sci Rep *7*, 4683.

Duncan, J.A., and Gilman, A.G. (1998). A Cytoplasmic Acyl-Protein Thioesterase That Removes Palmitate from G Protein α Subunits and p21RAS.

Ferguson, S.M., Brasnjo, G., Hayashi, M., Wolfel, M., Collesi, C., Giovedi, S., Raimondi, A., Gong, L.W., Ariel, P., Paradise, S.*, et al.* (2007). A selective activity-dependent requirement for dynamin 1 in synaptic vesicle endocytosis. Science *316*, 570-574.

Fogel, A.I., Li, Y., Giza, J., Wang, Q., Lam, T.T., Modis, Y., and Biederer, T. (2010). N-Glycosylation at the SynCAM (Synaptic Cell Adhesion Molecule) Immunoglobulin Interface Modulates Synaptic Adhesion.

Fogel, A.I., Stagi, M., Perez de Arce, K., and Biederer, T. (2011). Lateral assembly of the immunoglobulin protein SynCAM 1 controls its adhesive function and instructs synapse formation. Embo j *30*, 4728-4738.

Forrester, M.T., Hess, D.T., Thompson, J.W., Hultman, R., Moseley, M.A., Stamler, J.S., and Casey, P.J. (2010). Site-specific analysis of protein S-acylation by resin-assisted capture. J Lipid Res *52*, 393-398.

Fukata, M., Fukata, Y., Adesnik, H., Nicoll, R.A., and Bredt, D.S. (2004). Identification of PSD-95 palmitoylating enzymes. Neuron *44*, 987-996.

Fukata, Y., and Fukata, M. (2010). Protein palmitoylation in neuronal development and synaptic plasticity. Nat Rev Neurosci *11*, 161-175.

Goddard, A.D., and Watts, A. (2012). Regulation of G protein-coupled receptors by palmitoylation and cholesterol. In BMC Biol, p. 27.

Greaves, J., and Chamberlain, L.H. (2007). Palmitoylation-dependent protein sorting. J Cell Biol *176*, 249-254.

Greaves, J., Prescott, G.R., Gorleku, O.A., and Chamberlain, L.H. (2009). The fat controller: roles of palmitoylation in intracellular protein trafficking and targeting to membrane microdomains (Review). Molecular membrane biology *26*, 67-79.

Gupta, P., Soyombo, A.A., Atashband, A., Wisniewski, K.E., Shelton, J.M., Richardson, J.A., Hammer, R.E., and Hofmann, S.L. (2001). Disruption of PPT1 or PPT2 causes neuronal ceroid lipofuscinosis in knockout mice. Proc Natl Acad Sci U S A *98*, 13566-13571.

Hayashi, T., Rumbaugh, G., and Huganir, R.L. (2005). Differential regulation of AMPA receptor subunit trafficking by palmitoylation of two distinct sites. Neuron *47*, 709-723.

Hellsten, E., Vesa, J., Olkkonen, V.M., Jalanko, A., and Peltonen, L. (1996). Human palmitoyl protein thioesterase: evidence for lysosomal targeting of the enzyme and disturbed cellular routing in infantile neuronal ceroid lipofuscinosis. EMBO J *15*, 5240-5245.

Henderson, M.X., Wirak, G.S., Zhang, Y.-Q., Dai, F., Ginsberg, S.D., Dolzhanskaya, N., Staropoli, J.F., Nijssen, P.C.G., Lam, T.T., Roth, A.F.*, et al.* (2016). Neuronal ceroid lipofuscinosis with DNAJC5/CSPα mutation has PPT1 pathology and exhibit aberrant protein palmitoylation. Acta Neuropathologica *131*, 621-637.

Herguedas, B., Watson, J.F., Ho, H., Cais, O., García-Nafría, J., and Greger, I.H. (2019). Architecture of the heteromeric GluA1/2 AMPA receptor in complex with the auxiliary subunit TARP γ8.

Hinshaw, J.E. (2000). Dynamin and its role in membrane fission. Annu Rev Cell Dev Biol *16*, 483-519.

Hofmann, S.L., Lee, L.A., Lu, J.Y., and Verkruyse, L.A. (1997). Palmitoyl-protein thioesterase and the molecular pathogenesis of infantile neuronal ceroid lipofuscinosis. Neuropediatrics *28*, 27-30.

Huang, K., Yanai, A., Kang, R., Arstikaitis, P., Singaraja, R.R., Metzler, M., Mullard, A., Haigh, B., Gauthier-Campbell, C., Gutekunst, C.A.*, et al.* (2004). Huntingtin-interacting protein HIP14 is a palmitoyl transferase involved in palmitoylation and trafficking of multiple neuronal proteins. Neuron *44*, 977-986.

Itoh, S., Mizuno, K., Aikawa, M., and Aikawa, E. (2018). Dimerization of sortilin regulates its trafficking to extracellular vesicles. J Biol Chem *293*, 4532-4544.

Janda, C.Y., and Garcia, K.C. (2015). Wnt acylation and its functional implication in Wnt signalling regulation. Biochem Soc Trans *43*, 211-216.

Kanaani, J., Diacovo, M.J., El-Husseini Ael, D., Bredt, D.S., and Baekkeskov, S. (2004). Palmitoylation controls trafficking of GAD65 from Golgi membranes to axon-specific endosomes and a Rab5a-dependent pathway to presynaptic clusters. J Cell Sci *117*, 2001-2013.

Kang, R., Wan, J., Arstikaitis, P., Takahashi, H., Huang, K., Bailey, A.O., Thompson, J.X., Roth, A.F., Drisdel, R.C., Mastro, R.*, et al.* (2008). Neural palmitoyl-proteomics reveals dynamic synaptic palmitoylation. Nature *456*, 904-909.

Kim, S.J., Zhang, Z., Sarkar, C., Tsai, P.C., Lee, Y.C., Dye, L., and Mukherjee, A.B. (2008). Palmitoyl protein thioesterase-1 deficiency impairs synaptic vesicle recycling at nerve terminals, contributing to neuropathology in humans and mice. J Clin Invest *118*, 3075-3086.

Kim, Y., Yang, H., Min, J.K., Park, Y.J., Jeong, S.H., Jang, S.W., and Shim, S. (2018). CCN3 secretion is regulated by palmitoylation via ZDHHC22. Biochem Biophys Res Commun *495*, 2573-2578.

Kong, E., Peng, S., Chandra, G., Sarkar, C., Zhang, Z., Bagh, M.B., and Mukherjee, A.B. (2013). Dynamic palmitoylation links cytosol-membrane shuttling of acyl-protein thioesterase-1 and acyl-protein thioesterase-2 with that of proto-oncogene H-ras product and growth-associated protein-43. J Biol Chem *288*, 9112-9125.

Koster, K.P., and Yoshii, A. (2019). Depalmitoylation by Palmitoyl-Protein Thioesterase 1 in Neuronal Health and Degeneration. Front Synaptic Neurosci *11*.

Lehtovirta, M., Kyttala, A., Eskelinen, E.L., Hess, M., Heinonen, O., and Jalanko, A. (2001). Palmitoyl protein thioesterase (PPT) localizes into synaptosomes and synaptic vesicles in neurons: implications for infantile neuronal ceroid lipofuscinosis (INCL). Hum Mol Genet *10*, 69-75.

Lemonidis, K., Werno, M.W., Greaves, J., Diez-Ardanuy, C., Sanchez-Perez, M.C., Salaun, C., Thomson, D.M., and Chamberlain, L.H. (2015). The zDHHC family of S-acyltransferases. Biochem Soc Trans *43*, 217-221.

Li, Y., Hu, J., Höfer, K., Wong, A.M.S., Cooper, J.D., Birnbaum, S.G., Hammer, R.E., and Hofmann, S.L. (2010). DHHC5 Interacts with PDZ Domain 3 of Post-synaptic Density-95 (PSD-95) Protein and Plays a Role in Learning and Memory*. In J Biol Chem, pp. 13022-13031.

Lin, D.T., and Conibear, E. (2015). ABHD17 proteins are novel protein depalmitoylases that regulate N-Ras palmitate turnover and subcellular localization. Elife *4*, e11306.

Lin, D.T., Makino, Y., Sharma, K., Hayashi, T., Neve, R., Takamiya, K., and Huganir, R.L. (2009). Regulation of AMPA receptor extrasynaptic insertion by 4.1N, phosphorylation and palmitoylation. Nat Neurosci *12*, 879-887.

Liu, H., Yan, P., Ren, J., Wu, C., Yuan, W., Rao, M., Zhang, Z., and Kong, E. (2019). Identifying the Potential Substrates of the Depalmitoylation Enzyme Acyl-protein Thioesterase 1. Curr Mol Med *19*, 364-375.

Lu, J.Y., Verkruyse, L.A., and Hofmann, S.L. (1996). Lipid thioesters derived from acylated proteins accumulate in infantile neuronal ceroid lipofuscinosis: correction of the defect in lymphoblasts by recombinant palmitoyl-protein thioesterase.

Lyly, A., von Schantz, C., Salonen, T., Kopra, O., Saarela, J., Jauhiainen, M., Kyttala, A., and Jalanko, A. (2007). Glycosylation, transport, and complex formation of palmitoyl protein thioesterase 1 (PPT1)--distinct characteristics in neurons. BMC cell biology *8*, 22.

Magee, A.I., Gutierrez, L., McKay, I.A., Marshall, C.J., and Hall, A. (1987). Dynamic fatty acylation of p21N-ras. Embo j *6*, 3353-3357.

Mellacheruvu, D., Wright, Z., Couzens, A.L., Lambert, J.-P., St-Denis, N.A., Li, T., Miteva, Y.V., Hauri, S., Sardiu, M.E., Low, T.Y.*, et al.* (2013). The CRAPome: a contaminant repository for affinity purification–mass spectrometry data. Nature Methods *10*, 730-736.

Mitchell, D.A., Vasudevan, A., Linder, M.E., and Deschenes, R.J. (2006). Thematic review

series: Lipid Posttranslational Modifications. Protein palmitoylation by a family of DHHC protein S-acyltransferases.

Mitchison, H.M., Hofmann, S.L., Becerra, C.H., Munroe, P.B., Lake, B.D., Crow, Y.J., Stephenson, J.B., Williams, R.E., Hofman, I.L., Taschner, P.E.*, et al.* (1998). Mutations in the palmitoyl-protein thioesterase gene (PPT; CLN1) causing juvenile neuronal ceroid lipofuscinosis with granular osmiophilic deposits. Hum Mol Genet *7*, 291-297.

Miura, G.I., and Treisman, J.E. (2006). Lipid modification of secreted signaling proteins. Cell Cycle *5*, 1184-1188.

Montersino, A., and Thomas, G.M. (2015). Slippery Signaling: Palmitoylation-dependent Control of Neuronal Kinase Localization and Activity. Molecular membrane biology *32*, 179-188.

Naschberger, A., Orry, A., Lechner, S., Bowler, M.W., Nurizzo, D., Novokmet, M., Keller, M.A., Oemer, G., Seppi, D., Haslbeck, M.*, et al.* (2017). Structural Evidence for a Role of the Multi-functional Human Glycoprotein Afamin in Wnt Transport. Structure *25*, 1907-1915.e1905.

Newton, A.J., Kirchhausen, T., and Murthy, V.N. (2006). Inhibition of dynamin completely blocks compensatory synaptic vesicle endocytosis.

Ohyama, T., Verstreken, P., Ly, C.V., Rosenmund, T., Rajan, A., Tien, A.-C., Haueter, C., Schulze, K.L., and Bellen, H.J. (2007). Huntingtin-interacting protein 14, a palmitoyl transferase required for exocytosis and targeting of CSP to synaptic vesicles. The Journal of Cell Biology *179*, 1481-1496.

Pandya, N.J., Koopmans, F., Slotman, J.A., Paliukhovich, I., Houtsmuller, A.B., Smit, A.B., and Li, K.W. (2017). Correlation profiling of brain sub-cellular proteomes reveals co-assembly of synaptic proteins and subcellular distribution. Scientific Reports *7*, 1-11.

Ponimaskin, E., Dityateva, G., Ruonala, M.O., Fukata, M., Fukata, Y., Kobe, F., Wouters, F.S., Delling, M., Bredt, D.S., Schachner, M.*, et al.* (2008). Fibroblast Growth Factor-Regulated Palmitoylation of the Neural Cell Adhesion Molecule Determines Neuronal Morphogenesis. In J Neurosci, pp. 8897-8907.

Qiao, X., Lu, J.-Y., and Hofmann, S.L. (2007). Gene expression profiling in a mouse model of infantile neuronal ceroid lipofuscinosis reveals upregulation of immediate early genes and mediators of the inflammatory response. BMC Neuroscience *8*, 95.

Ren, J., Wen, L., Gao, X., Jin, C., Xue, Y., and Yao, X. (2008). CSS-Palm 2.0: an updated software for palmitoylation sites prediction. Protein engineering, design & selection : PEDS *21*, 639-644.

Romancino, D.P., Buffa, V., Caruso, S., Ferrara, I., Raccosta, S., Notaro, A., Campos, Y., Noto, R., Martorana, V., Cupane, A.*, et al.* (2018). Palmitoylation is a post-translational modification of Alix regulating the membrane organization of exosome-like small extracellular vesicles. Biochim Biophys Acta Gen Subj *1862*, 2879-2887.

Royle, S.J., and Lagnado, L. (2010). Clathrin-mediated endocytosis at the synaptic terminal: bridging the gap between physiology and molecules. Traffic *11*, 1489-1497.

Saheki, Y., and De Camilli, P. (2012). Synaptic Vesicle Endocytosis. In Cold Spring Harb Perspect Biol.

Sapir, T., Segal, M., Grigoryan, G., Hansson, K.M., James, P., and Reiner, O. (2019). The Interactome of Palmitoyl-Protein Thioesterase 1 (PPT1) Affects Neuronal Morphology and Function. Front Cell Neurosci *13*.

Segal-Salto, M., Hansson, K., Sapir, T., Kaplan, A., Levy, T., Schweizer, M., Frotscher, M., James, P., and Reiner, O. (2017). Proteomics insights into infantile neuronal ceroid lipofuscinosis (CLN1) point to the involvement of cilia pathology in the disease. Hum Mol Genet *26*, 1678.

Shipston, M.J. (2011). Ion channel regulation by protein palmitoylation. J Biol Chem *286*, 8709-8716.

Sialana, F.J., Gulyassy, P., Majek, P., Sjostedt, E., Kis, V., Muller, A.C., Rudashevskaya, E.L., Mulder, J., Bennett, K.L., and Lubec, G. (2016). Mass spectrometric analysis of synaptosomal membrane preparations for the determination of brain receptors, transporters and channels. Proteomics *16*, 2911-2920.

Sleat, D.E., Tannous, A., Sohar, I., Wiseman, J.A., Zheng, H., Qian, M., Zhao, C., Xin, W., Barone, R., Sims, K.B*., et al.* (2017). Proteomic Analysis of Brain and Cerebrospinal Fluid from the Three Major Forms of Neuronal Ceroid Lipofuscinosis Reveals Potential Biomarkers. J Proteome Res *16*, 3787-3804.

Tyynela, J., Palmer, D.N., Baumann, M., and Haltia, M. (1993). Storage of saposins A and D in infantile neuronal ceroid-lipofuscinosis. FEBS Lett *330*, 8-12.

Umbach, J.A., Zinsmaier, K.E., Eberle, K.K., Buchner, E., Benzer, S., and Gundersen, C.B. (1994). Presynaptic dysfunction in drosophila csp mutants. Neuron *13*, 899-907.

Vartak, N., Papke, B., Grecco, H.E., Rossmannek, L., Waldmann, H., Hedberg, C., and Bastiaens, P.I. (2014). The autodepalmitoylating activity of APT maintains the spatial organization of palmitoylated membrane proteins. Biophys J *106*, 93-105.

Verstreken, P., Koh, T.W., Schulze, K.L., Zhai, R.G., Hiesinger, P.R., Zhou, Y., Mehta, S.Q., Cao, Y., Roos, J., and Bellen, H.J. (2003). Synaptojanin is recruited by endophilin to promote synaptic vesicle uncoating. Neuron *40*, 733-748.

Vesa, J., Hellsten, E., Verkruyse, L.A., Camp, L.A., Rapola, J., Santavuori, P., Hofmann, S.L., and Peltonen, L. (1995). Mutations in the palmitoyl protein thioesterase gene causing infantile neuronal ceroid lipofuscinosis. Nature *376*, 584-587.

Virmani, T., Gupta, P., Liu, X., Kavalali, E.T., and Hofmann, S.L. (2005). Progressively reduced synaptic vesicle pool size in cultured neurons derived from neuronal ceroid lipofuscinosis-1 knockout mice. Neurobiol Dis *20*, 314-323.

Wei, H., Zhang, Z., Saha, A., Peng, S., Chandra, G., Quezado, Z., and Mukherjee, A.B. (2011). Disruption of adaptive energy metabolism and elevated ribosomal p-S6K1 levels contribute to INCL pathogenesis: partial rescue by resveratrol. Hum Mol Genet *20*, 1111-1121.

Yokoi, N., Fukata, Y., Sekiya, A., Murakami, T., Kobayashi, K., and Fukata, M. (2016). Identification of PSD-95 Depalmitoylating Enzymes. In J Neurosci, pp. 6431-6444.

Yu, R., Liu, H., Peng, X., Cui, Y., Song, S., Wang, L., Zhang, H., Hong, A., and Zhou, T. (2017). The palmitoylation of the N-terminal extracellular Cys37 mediates the nuclear translocation of VPAC1 contributing to its anti-apoptotic activity. Oncotarget *8*, 42728-42741.

Zhang, Y.-Q., Henderson, M.X., Colangelo, C.M., Ginsberg, S.D., Bruce, C., Wu, T., and Chandra, S.S. (2012). Identification of CSPα clients reveals a role in dynamin 1 regulation. Neuron *74*, 136-150.

Zinsmaier, K.E., Eberle, K.K., Buchner, E., Walter, N., and Benzer, S. (1994). Paralysis and early death in cysteine string protein mutants of Drosophila. Science (New York, NY) *263*, 977-980.

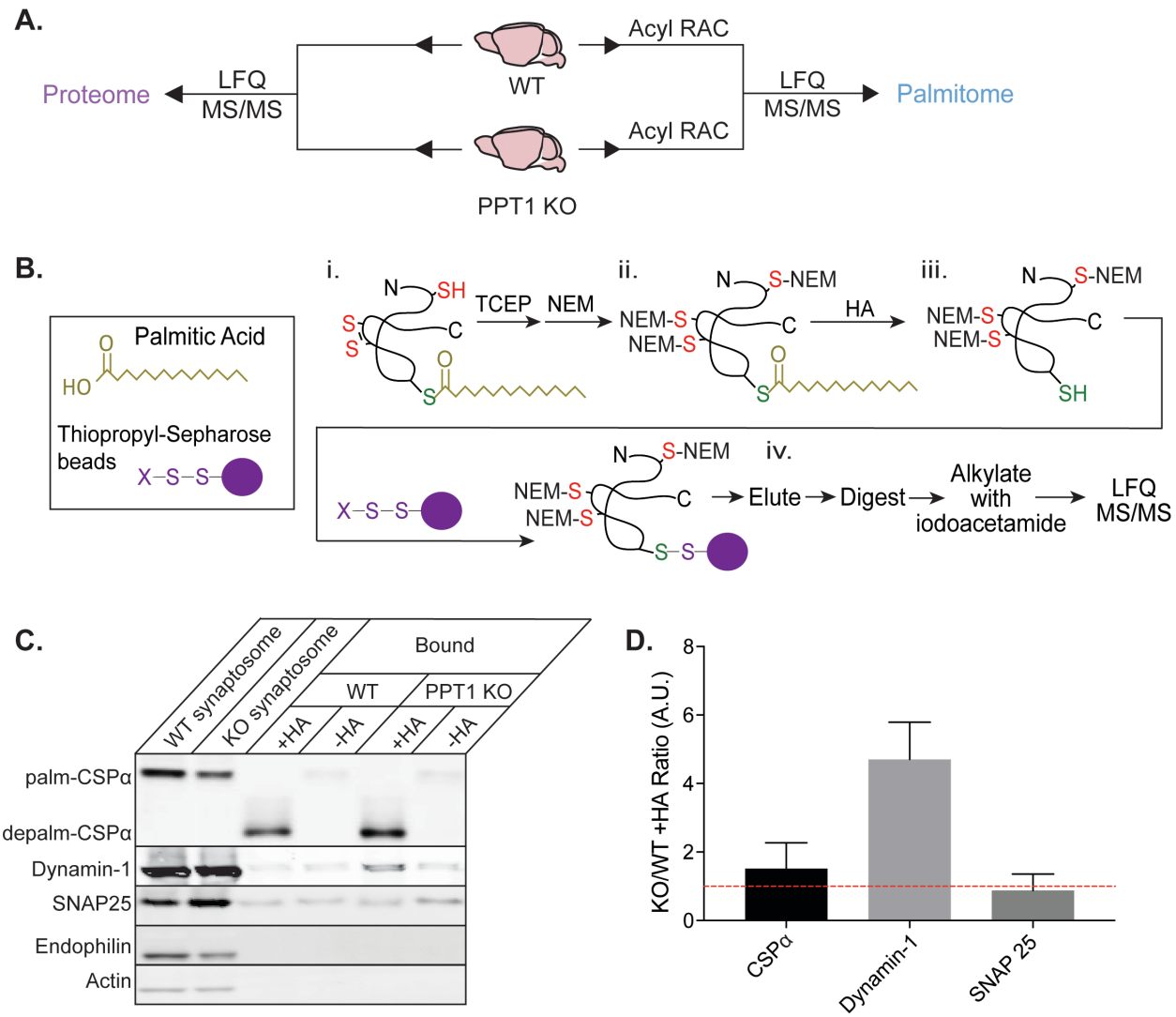

Figure 1. Overview of PPT1 substrate identification workflow. A) WT and PPT1 KO whole brains were prepared and proteins were isolated for proteomic analysis by Label-Free Quantification Mass Spectrometry (LFQ MS/MS) to identify overall protein expression (proteome; left) or following Acyl Resin-Assisted Capture (Acyl RAC) to identify palmitoylated proteins (palmitome; right). B) Schematic of Acyl RAC. i. Disulfide bonds were reduced with TCEP and residual thiol groups were blocked with NEM. ii. Hydroxylamine (HA) hydrolyzes palmitate groups, leaving behind an unblocked free thiol. iii. Free thiols bind to thiopropyl sepharose beads allowing for isolation of palmitoylated proteins. iv. These proteins were then eluted from beads with DTT, digested and alkylated with iodoacetamide for LFQ MS/MS analysis. The same experimental scheme was conducted on synaptosomes. C) Pull-down and immunoblotting of proteins from synaptosomes that were palmitoylated. Addition of HA allowed CSPα, Dynamin-1, and SNAP-25, all of which are palmitoylated proteins, to be pulled down on thiopropyl sepharose beads, but not endophilin or actin, which are not palmitoylated. Note that addition of HA removes palmitate and causes a molecular weight shift of palmitoylated CSPα to depalmitoylated CSPα. D) Quantification of western blotting of +HA bands, plotted as a ratio of KO/WT. CSPα is a known PPT1 substrate and shows elevated palmitoylation in KO/WT, while SNAP-25 does not. Based on this, we set 1.5-fold as a cut-off for identifying significant PPT1 substrates.

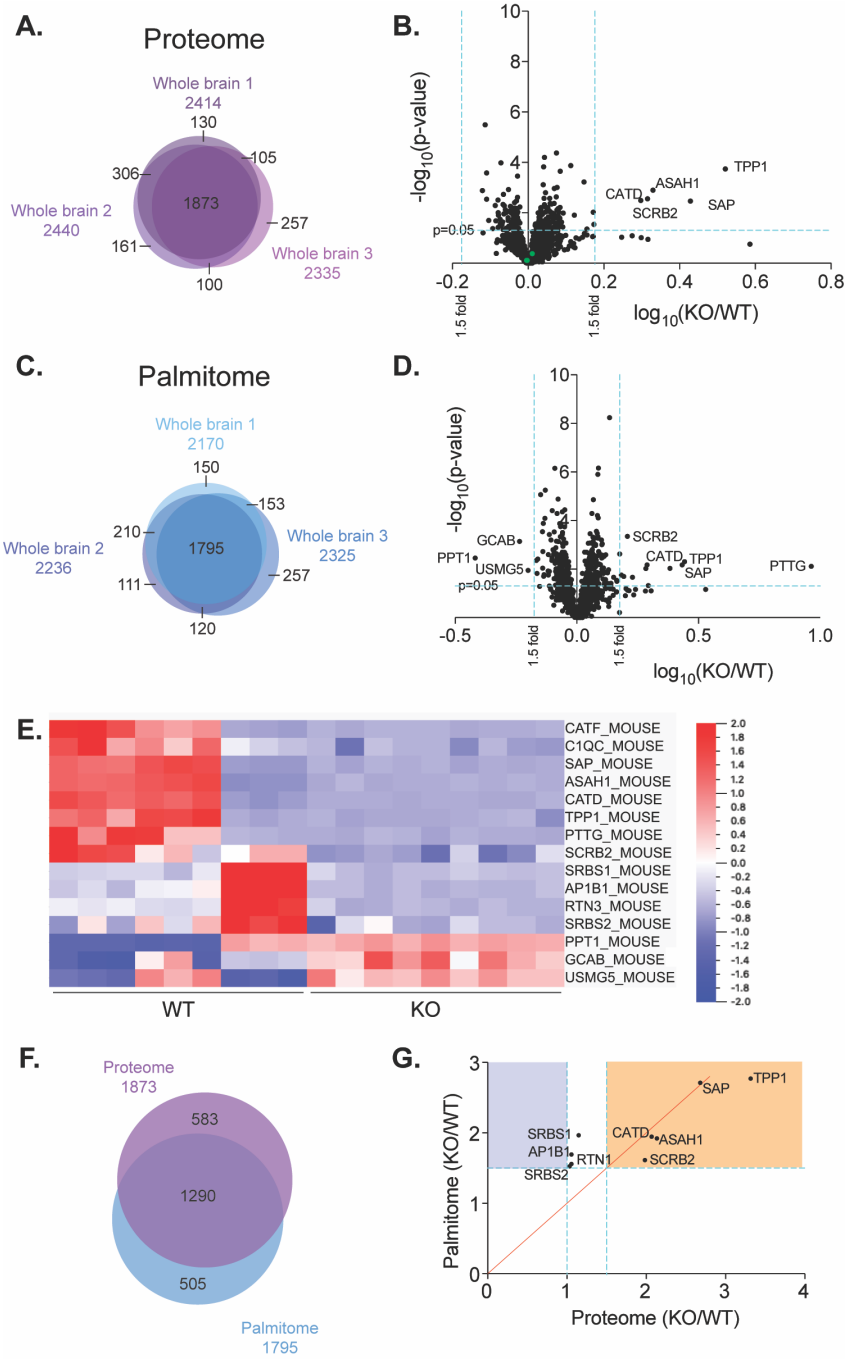

Figure 2. PPT1 KO results in few measurable palmitoylation changes in whole brain. A) Venn diagram of 3 independent proteome experiments identified 1873 common proteins. B) Volcano plot of the fold change between genotypes (KO/WT) for the proteins identified in all 3 biological replicates. The p-value was calculated using a two-tailed t-test on 3 biological and 3 technical replicates. While the technical replicates do not meet the t-test condition for independence, we chose to proceed in this manner in order to generate more putative substrates that could later be validated with higher stringency. 5 proteins had significantly changed protein expression (1.5-fold, P<0.05; blue lines). Other depalmitoylating enzymes (green points) do not show compensatory changes in protein expression. C) Venn diagram of 3 palmitome experiments identified 1795 common proteins. D) Volcano plot indicating that 15 proteins had significantly changed palmitoylation levels in whole brain (3 decrease, including PPT1; 12 increase; 1.5-fold, P<0.05; blue lines). E) Heat map of palmitoylation levels of

significantly changed proteins for each experiment (3 biological, 3 technical replicates per genotype). F) Venn diagram of 1290 common proteins identified in whole brain proteome and palmitome (n=3 each). G) Protein expression levels compared to palmitoylation levels for significantly changed proteins in palmitome. Proteins in orange region had significant increases (1.5-fold, $P<0.05$) in both the proteome and palmitome. Proteins in blue region had decreased or unchanged protein expression and increased palmitoylation. Red line indicates equal expression and palmitoylation levels (x=y).

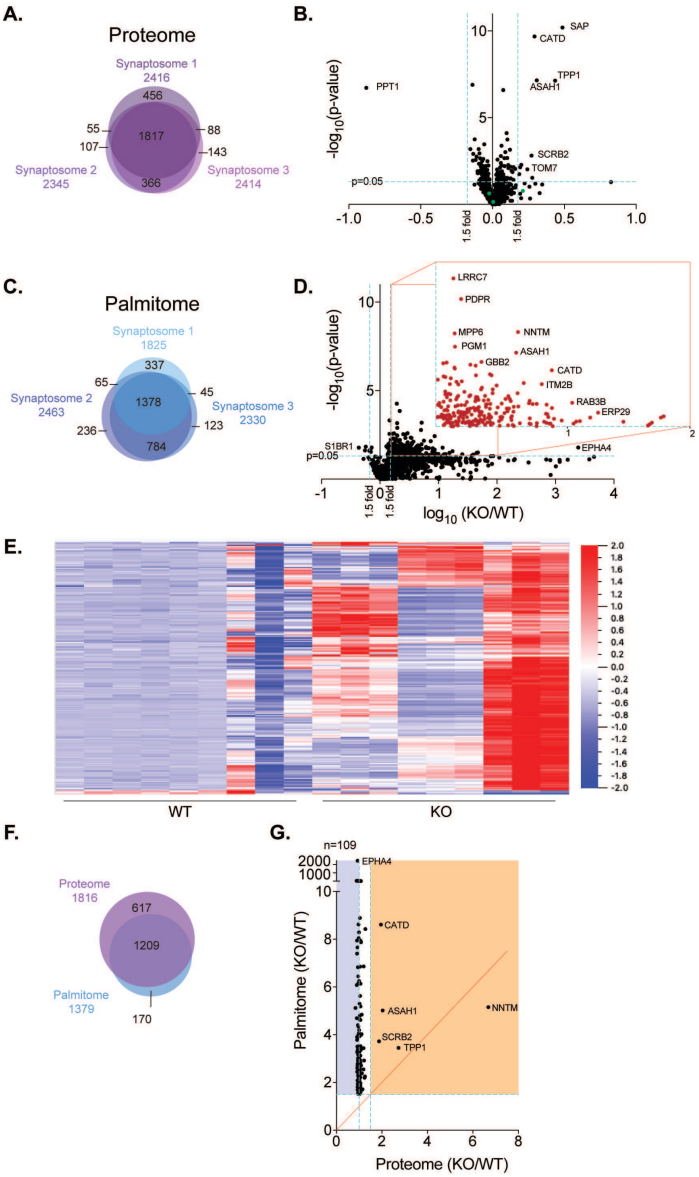

Figure 3. PPT1 KO results in significant changes in the synaptic palmitome. A) Venn diagram of 3 independent proteome experiments identified 1817 common proteins. B) Volcano plot of the fold change between genotypes (KO/WT) for the proteins identified in all 3 biological replicates. 11 proteins had significantly changed protein expression (1 decrease (PPT1); 10 increase; 1.5-fold, P<0.05; blue lines). Other depalmitoylating enzymes (green points) did not show significant compensatory changes in protein expression. C) Venn diagram of 3 palmitome experiments identified 1378 common proteins. D) Volcano plot indicates 242 proteins had significantly changed palmitoylation levels (4 decrease; 238 increase; 1.5-fold, P<0.05; blue lines). Inset shows significantly increased proteins. E) Heat map of palmitoylation levels of significantly changed proteins for each experiment (3 biological, 3 technical replicates per genotype). F) Venn diagram of 1209 common proteins identified in whole brain proteome and palmitome (n=3 each). G) Protein expression levels compared to palmitoylation levels for significantly changed proteins in palmitome. Proteins in orange region had increases (1.5-fold, P<0.05) to both proteome and palmitome. Proteins in blue region had decreased or unchanged protein expression and increased palmitoylation. Red line indicates equal expression and palmitoylation levels (x=y). While NNTM has a high fold change, it does not meet the p-value criteria for significantly increased protein expression (p=0.0522), and is therefore excluded from this category.

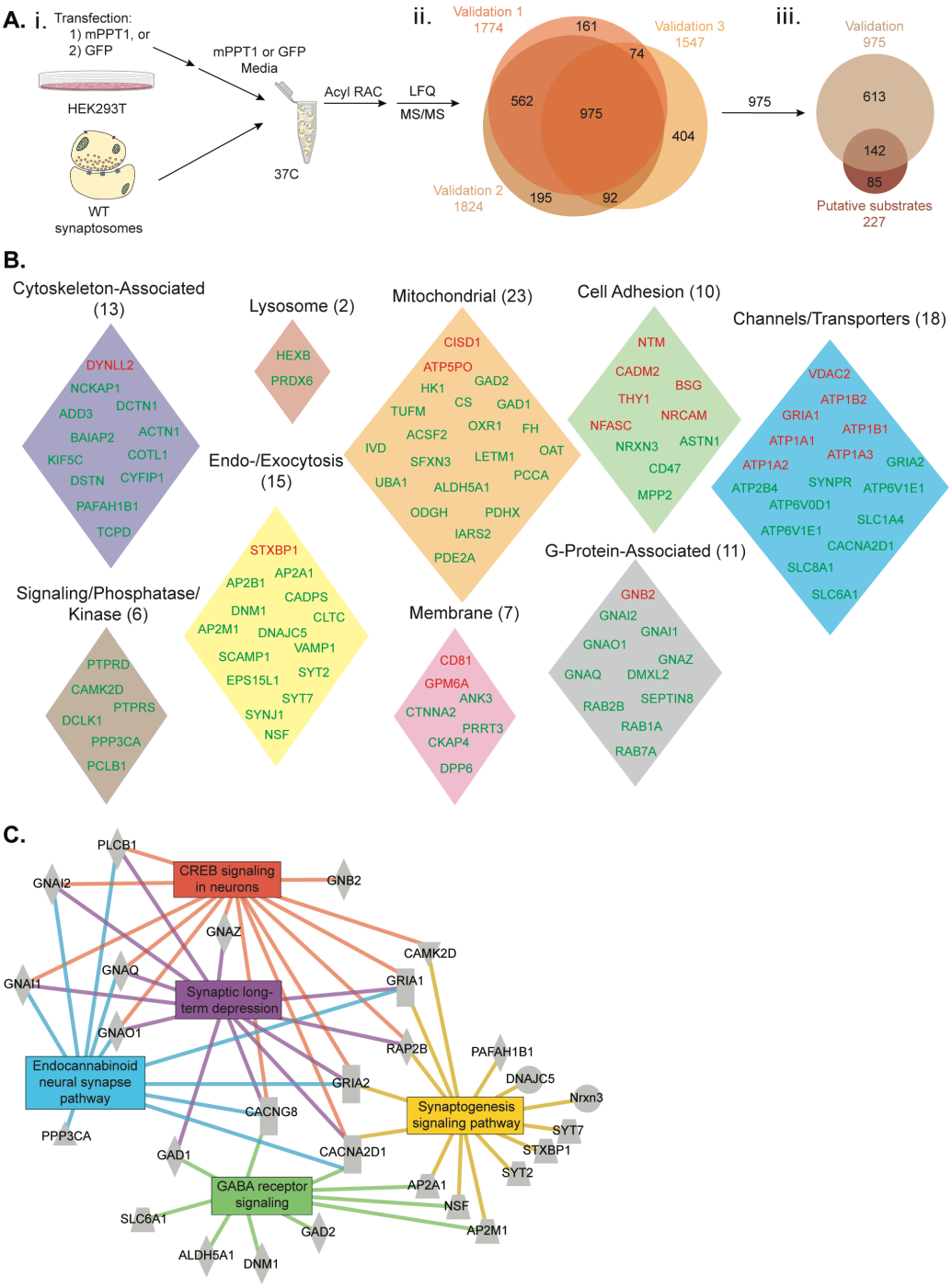

Figure 4. PPT1 substrates can be depalmitoylated directly by recombinant mPPT1. A) i. Schematic of PPT1-mediated depalmitoylation assay. ii. Venn diagram of PPT1-mediated depalmitoylation assay (n=3 biological replicates, n=3 technical replicates) shows 975 proteins common to replicates. iii. Comparison of PPT1-mediated depalmitoylation proteins to putative substrates revealed 142 validated PPT1 substrates. B) The 142 combined high- (red) and medium- (green) confidence validated proteins fall into curated UniProt functional and subcellular location groupings. C) Ingenuity pathway analysis identified enrichment of high- and medium- confidence substrates for synaptic long-term depression, synaptogenesis signaling, GABA receptor signaling, endocannabinoid neural synapses, and CREB signaling in neurons.

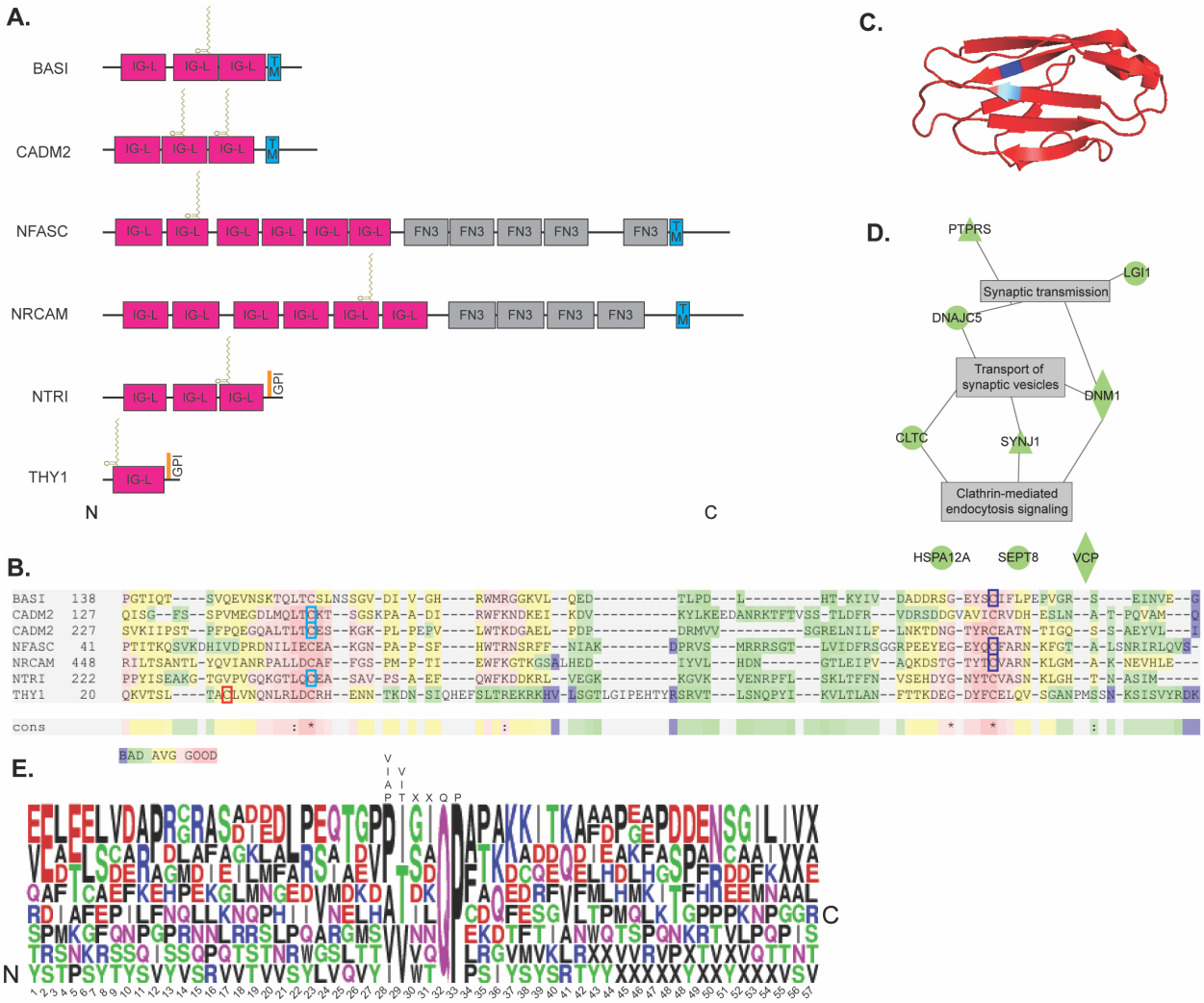

Figure 5. PPT1 recognizes certain classes of substrates through select motifs. A) Domain organization of IgG domain-containing synaptic adhesion molecules with palmitoylation sites represented as lipid chains. IG-L – Ig-like; FN3 – fibronectin 3; TM – transmembrane. B) IgG domain-containing synaptic adhesion molecules show high homology surrounding the palmitoylated cysteines (boxed). Red indicates high homology; green indicates low homology. The two conserved cysteines at the N- (**Figure 5B**, light blue) and C- termini (**Figure 5B**, dark blue) of this domain are both identified as carbamidomethylated in different experiments. C) Representative IgG domain structure (CADM1; PDB, 3M45) with position of palmitoylated cysteine highlighted in blue. D) Ingenuity pathway analysis of DHHC17 motif-containing proteins identifies clathrin-mediated endocytosis signaling as the top enriched pathway. These pathways account for 6 of the 9 motif-containing proteins. E) Alignment of DHHC17 recognition motif for the 9 PPT1 substrates with 26 amino acids on either side of the motif. The motif is noted above the logo. There are no other motifs surrounding the DHHC17 motif.

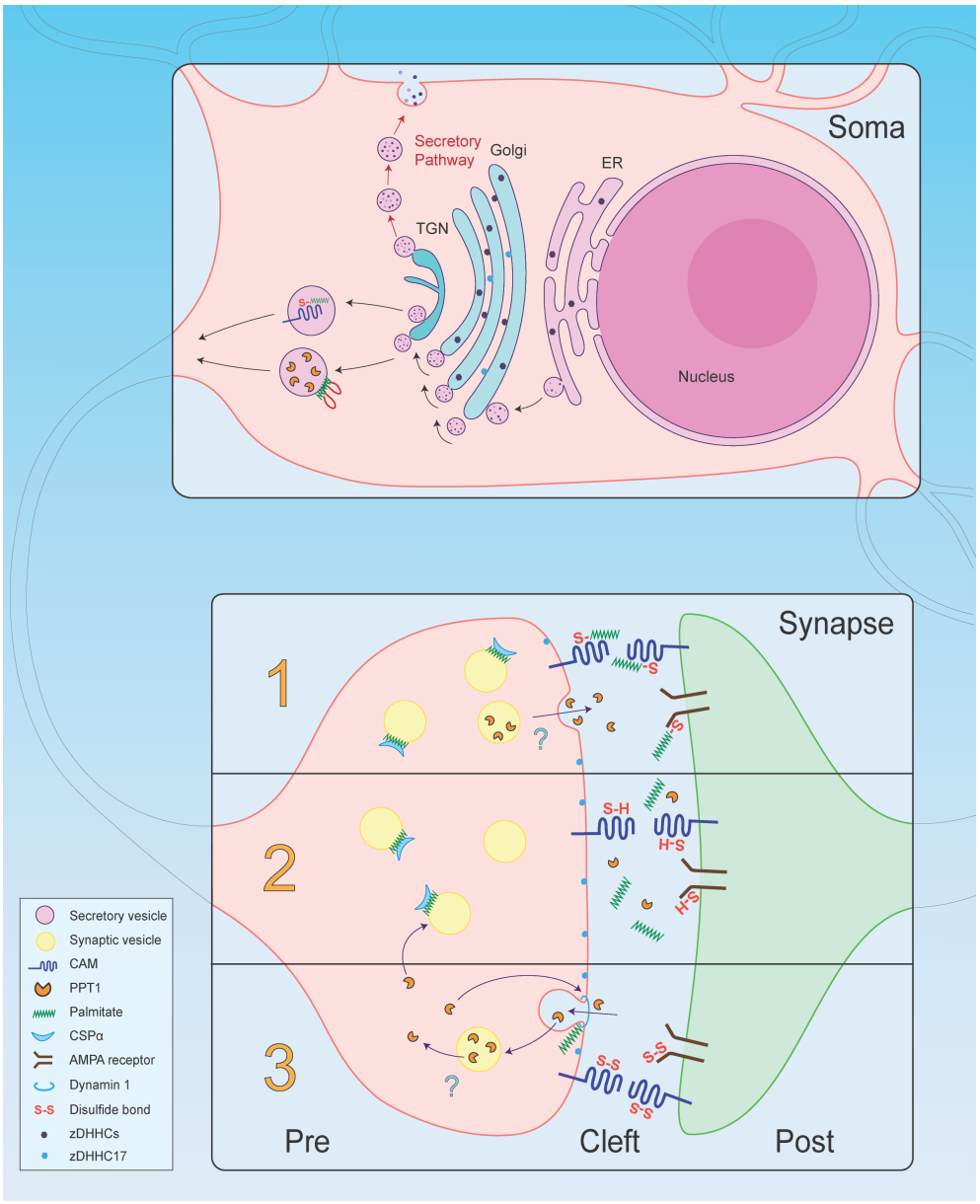

Figure 6. Functions of synaptic depalmitoylation by PPT1. Palmitoylation of synaptic cell adhesion molecules co-translationally in the lumen of the ER or Golgi, while for cytosolic synaptic proteins occurs on the surface of the Golgi (top panel). We propose that somatic palmitoylation keep synaptic proteins inert, in addition to be important for sorting and trafficking. For example, palmitoylation may prevent aberrant adhesion interactions during trafficking to the cleft (top panel). Our data suggest that PPT1 is trafficked through the secretory pathway and secreted at synaptic termini (1), where it can reach and depalmitoylate its substrates on either side of the synaptic cleft (2). Once depalmitoylated, these substrates form disulfide bonds in the oxidizing environment of the cleft (3). PPT1 may depalmitoylate its cytosolic pre-synaptic substrates following re-endocytosis, or an alternate pool of PPT1 may depalmitoylate these substrates. Many of these cytosolic PPT1 substrates are palmitoylated locally by the plasma membrane zDHHC17, allowing for local cycles of palmitoylation and depalmitoylation.